

Incorporation of Graphenes in Nanostructured TiO₂ Films via Molecular-Grafting for Dye-Sensitized Solar Cell Application

Yong-Bing Tang,^{1,2,3} Chun-Sing Lee,^{1,*} Jun Xu,¹ Zeng-Tao Liu,¹ Zhen-Hua Chen,¹ Zhubing He,¹ Yu-Lin Cao,¹ Guodong Yuan,¹ Haisheng Song,¹ Limiao Chen,¹ Linbao Luo,¹ Hui-Ming Cheng,² Wen-Jun Zhang,¹ Igor Bello,¹ Shuit-Tong Lee^{1,3,*}

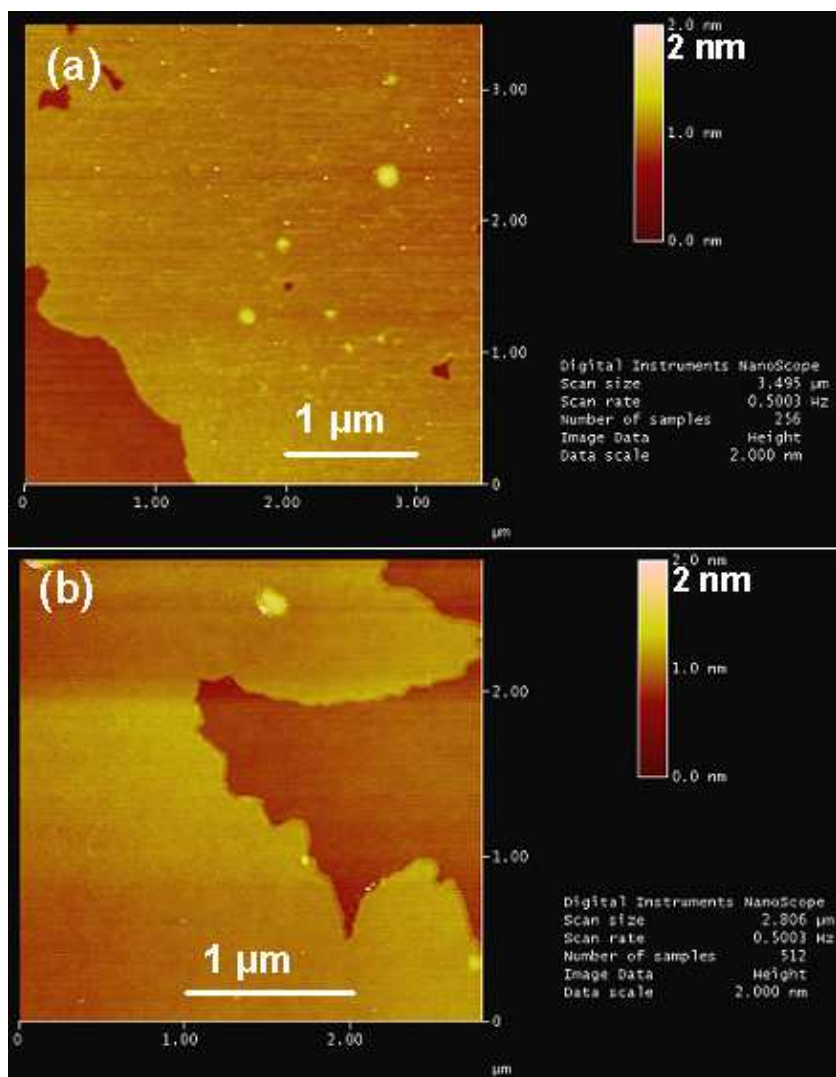
¹Center of Super-Diamond and Advanced Films (COSDAF) and Department of Physics and Materials Science, City University of Hong Kong, Hong Kong SAR, P. R. China, Shenyang National Laboratory for Materials Science (SYNL),
²Institute of Metal Research (IMR), Chinese Academy of Sciences, Shenyang 110016, P. R. China, ³Functional Nano & Soft Materials Laboratory (FUNSOM), Soochow University, Suzhou, Jiangsu 215123, P. R. China

Supporting Information

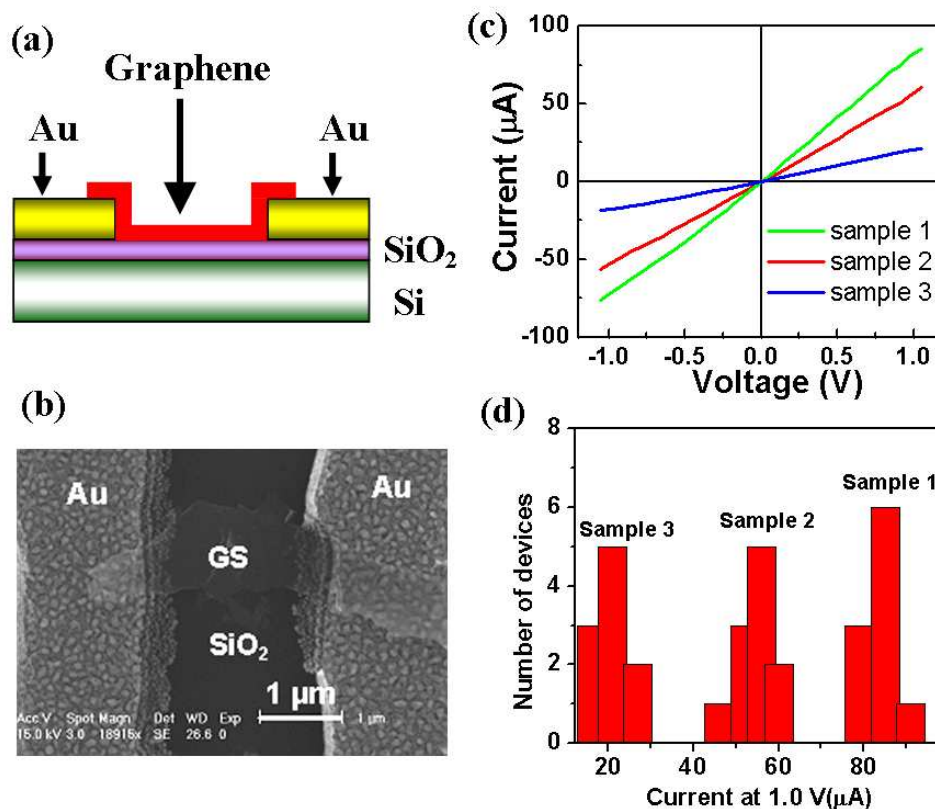
1. AFM characteristics
2. *I-V* measurements of the reduced GS prepared by different oxidation times
3. XPS spectra of GO precursors and reduced GS from samples 1-3
4. SEM images of the attachment of TiO₂ nanoparticles on graphene sheets
5. Typical HeI UPS spectrum of the reduced graphene sheets.
6. Schematic structure of the DSSCs
7. Resistivity of GS/TiO₂ films as a function of GS concentration
8. Transmittance spectra and photograph image of GS/TiO₂ films deposited from different GS concentrations

*Address correspondence to apcslee@cityu.edu.hk and apannale@cityu.edu.hk

1. Figure S1: AFM images indicate that the as-prepared graphene sheets have a relatively flat and planar structure, similar to that obtained by micromechanical cleavage,¹ and consist of up to 80% single-layer graphene. Most of graphene sheets have a lateral size on the order of micrometers.



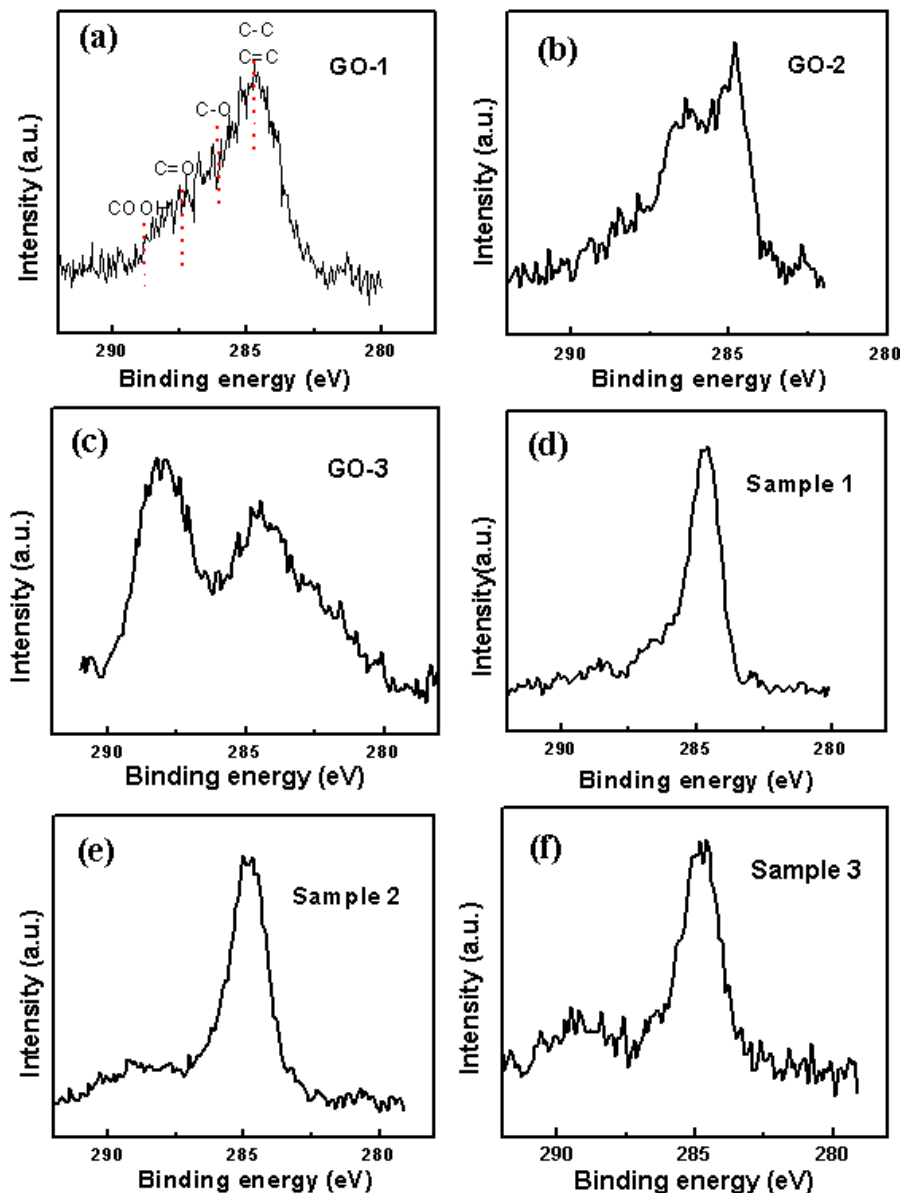
2. Figure S2. (a) Schematic of the two-terminal devices based on individual graphene on Si-SiO₂(300 nm) substrates between a pair of parallel Au (~30 nm) electrodes spaced ~2 μm. (b) SEM image of a typical two-terminal device. (c) Representative *I-V* curves for each sample. (d) Statistical histogram of the current response at 1.0 V for each sample.



To investigate the conductivity of the reduced GS prepared by different oxidation times, we fabricated two-terminal devices based on individual graphene by dropping the GS suspension on Si-SiO₂ substrates between a pair of parallel Au (~30 nm) electrodes spaced ~2 μm (schematically illustrated in Fig. S2a). The first experiment is a comparison of the conductivity difference between the samples prepared by different oxidation times. A representative example of one of the devices tested is depicted in Fig. S2(b). Figure S2(c) shows the representative *I-V* curves for each sample. The results show the conductivity decreased from sample 1 to sample 3. To statistically evaluate the electrical properties, we have fabricated and measured at

least 10 devices based on single GS from each sample. We stress that most of transport measurements showed good reproducibility, ascertaining the reliability of results. Figure S2(d) shows the statistical histogram of the current response at 1.0 V. It can be seen that the current at 1.0 V for sample 1 is in the range of 78–91 μA , whereas the conductivity decreases to 46–59 μA for sample 2, and 16–27 μA for sample 3. The above results clearly show the conductivity of reduced GS decreased by increasing oxidation time during the chemical exfoliation process. One possible reason for such conductivity reduction could be attributed to increase of residual oxygen-containing groups with increasing oxidation time.

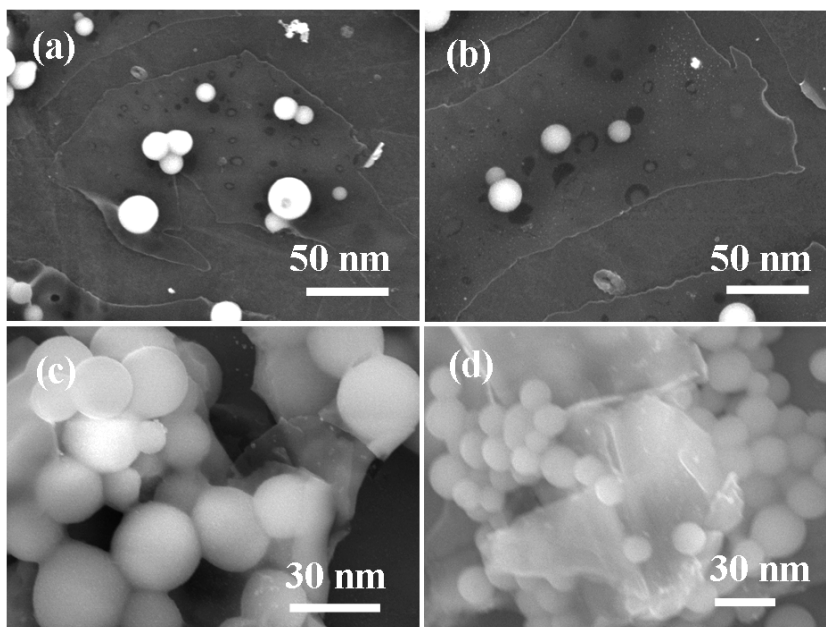
3. **Figure S3** (a-c) The C 1s peaks in the XPS spectra of GO precursors from samples 1-3. (d-f) C 1s peaks in the XPS spectra of reduced GS from samples 1-3.



We performed x-ray photoemission spectroscopy (XPS) measurements to provide further evidence that increasing oxidation time increased the number of residual oxygen-containing groups. The carbon 1s spectra of the GO precursors from samples 1-3 showed that the carbon-oxygen related signals (C-O at 286 eV, C=O at 287 eV, and COOH at 288 eV) become more obvious with increasing oxidation time, which demonstrates that the increase of oxidation time leads to more complete oxidation of

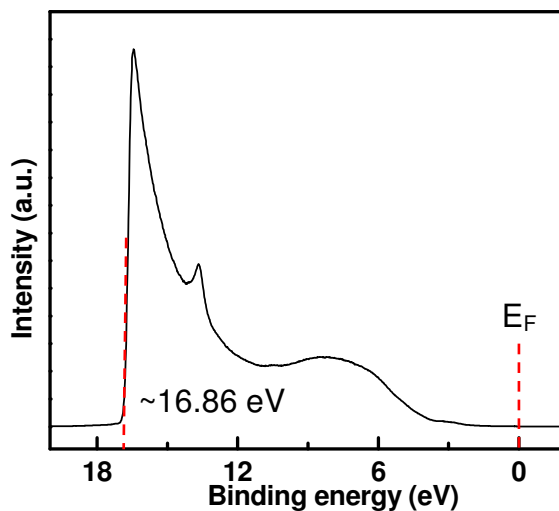
graphite flakes. For sample 1, the corresponding C 1s peak structure of the reduced GS is similar to that of pristine HOPG,² without significant signals corresponding to the C–O species of GO (Fig. S2d). However, the signals assigned to C–O groups gradually increased in sample 2 and sample 3 (Fig. S3e, f). These results suggest that the number of residual oxygen-containing groups in the final graphene sheets is increased by increasing the oxidation time.

4. Figure S4 SEM images of the attachment of TiO₂ nanoparticles to graphene sheets for sample 1(a,b), sample 2 (c), and sample 3 (d).



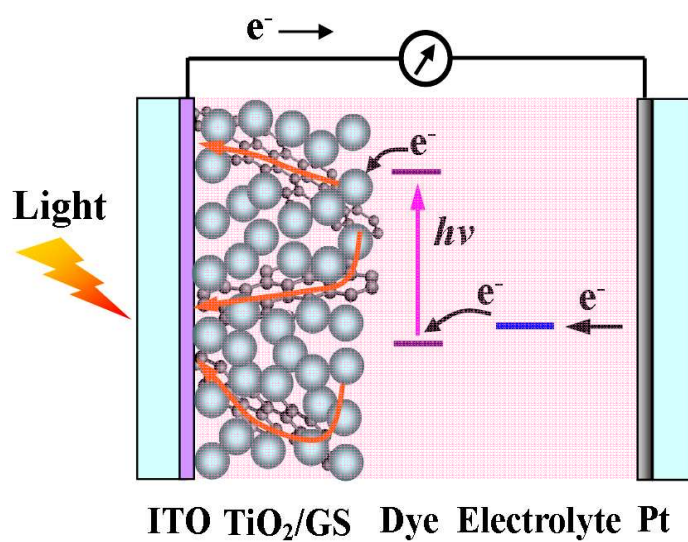
It was found that the attachment of TiO₂ nanoparticles on GS is not significant in sample 1 (Fig. S4a, b) with only 5 hours oxidation, but the attachment of TiO₂ nanoparticles is considerable in samples 2 and 3 with oxidation times higher than 10 hours (Fig. S4c, d). Combining this with the above XPS results, we deduce that the good attachment of TiO₂ nanoparticles in samples 2 and 3 is due to the increase of residual oxygen-containing groups with long oxidation process.

5. Figure S5 Typical HeI UPS spectrum of the reduced graphene sheets.

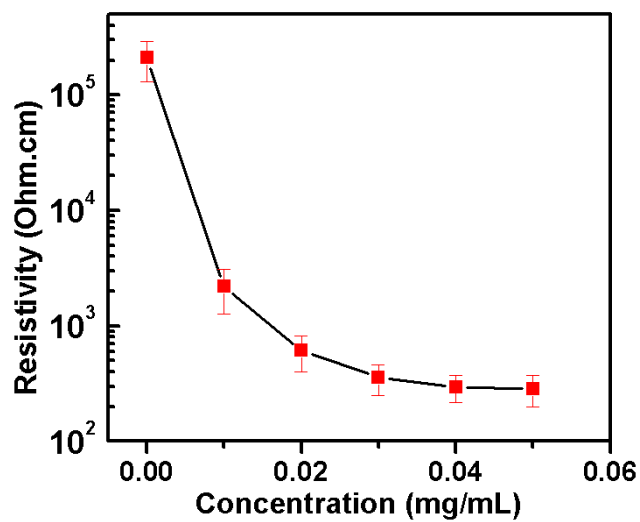


We measured the work function of the reduced GS films by ultraviolet photoemission spectroscopy (UPS) at 21.22 eV ($h\nu$) with a resolution of 20 meV using a VG ESCALAB 220i-XL ultrahigh vacuum (UHV) surface analysis system.³ Prior to measurement, GS suspensions were dip-coated on Si substrates and then dried at room temperature. Meanwhile, Si substrates without GS film were also measured to eliminate the influence from the substrate. Figure S5 shows the typical HeI UPS spectrum of the chemically reduced GS film. It can be seen that the high binding energy (BE) edge is at 16.86 eV. Based on this value, the work function (Φ) was then obtained from $h\nu=BE+\Phi$ to be about 4.36 eV. This value is close to the work function of pristine GS (~ 4.5 eV), indicating that the residual oxygen containing groups did not change much the work function of GS.

6. Figure S6 Schematic structure of the DSSCs with an active cell area of 0.5×0.5 cm^2 .

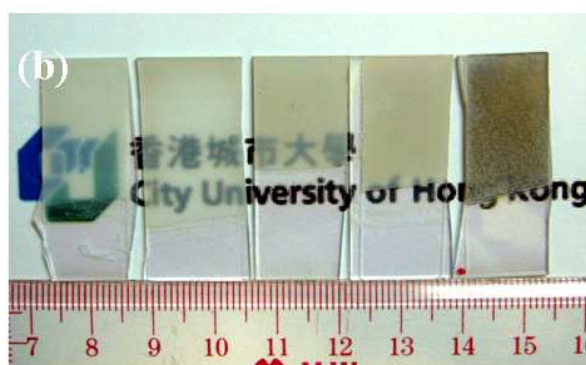
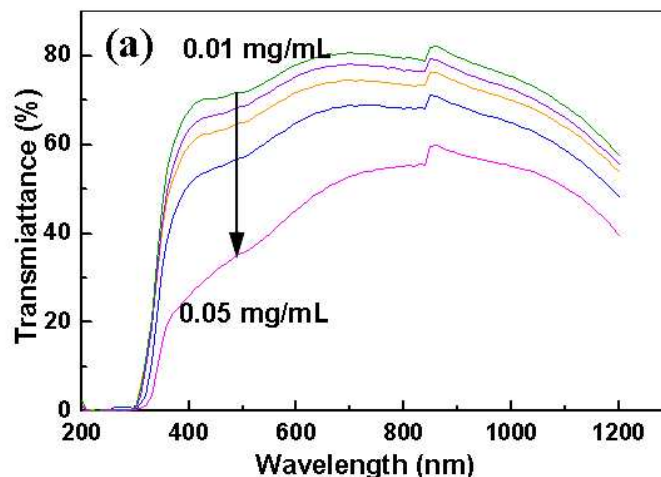


7. Figure S7. Resistivity of GS/TiO₂ films as a function of GS concentration.



The resistivity of GS/TiO₂ films decreases continuously with increasing GS concentration and approaches $2.85 \pm 0.87 \times 10^2 \Omega \cdot \text{cm}$ at GS concentration of 0.05 mg/mL.

8. Figure S8 (a) Transmittance spectra of the composite films deposited from different GS concentrations as indicated. (b) Photograph image of the corresponding GS/TiO₂ films deposited on ITO glasses (GS concentration increases from 0.01 (left) to 0.05 mg/mL (right)).



Increase of GS concentration leads to a decrease of the transmittance of visible light through the composite films, also reported previously,⁴⁻⁶ in which the transmittance of GS films decreased with increasing film thickness. Figure S8(a) shows the transmittance spectra and the corresponding photograph image (b) of GS/TiO₂ composite films prepared from different GS concentrations. It can be seen that the decrease in the transmittance is obvious with increasing GS concentration to 0.05 mg/mL, which may be due to too many GS in the composite film.⁴⁻⁶

References:

1. Novoselov, K. S.; Geim, A. K.; Morozov, S. V.; Jiang, D.; Zhang, Y.; Dubonos, S. V.; Grigorieva, I.V.; Firsov, A. A. Electric Field Effect in Atomically Thin Carbon Films. *Science* **2004**, *306*, 666-669.
2. Li, X. L.; Zhang, G. Y.; Bai, X. D.; Sun, X. M.; Wang, X. R.; Wang, E. G.; Dai, H. J. Highly Conducting Graphene Sheets and Langmuir-Blodgett Films. *Nat. Nanotech.* **2008**, *3*, 538-542.
3. Tang, J. X.; Zhou, Y. C.; Liu, Z. T.; Lee, C. S.; Lee, S. T. Interfacial Electronic Structures in An Organic Double-Heterostructure Photovoltaic Cell. *Appl. Phys. Lett.* **2008**, *93*, 043512.
4. Wang, X.; Zhi, L. J.; Tsao, N.; Tomovic, Z.; Li, J.; Mullen, K. Transparent Carbon Films as Eelectrodes in Organic Solar Cells. *Angew. Chem. Int. Ed.* **2008**, *47*, 2990-2992.
5. Wang, X.; Zhi, L.; Mullen, K. Transparent, Conductive Graphene Electrodes for Dye-Sensitized Solar Cells. *Nano Lett.* **2008**, *8*, 323-327.
6. Z. F. Liu, Q. Liu, Y. Huang, Y. F. Ma, S. G. Yin, X. Y. Zhang, W. Sun, Y. S. Chen, Organic Photovoltaic Devices Based on a Novel Acceptor Material: Graphene. *Adv. Mater.* **2008**, *20*, 3924.